Phase instability and local dynamics in directional solidification

A. Ghazali
Groupe de Physique des Solides, Universités Paris 6 et 7, 2 place Jussieu, 75251 Paris CEDEX 05, France

C. Misbah
Institut Max von Laue-Paul Langevin, Boîte Postale 156, 38042 Grenoble CEDEX 9, France
(Received 13 April 1992)

Recently a general phase equation has been derived from the boundary integral equation, and preliminary results on the Eckhaus instability were given [K. Brattkus and C. Misbah, Phys. Rev. Lett. **64**, 1935 (1990)]. The first focus of the present study is devoted to an extensive analysis of both the derivation of the phase equation and the computation of the Eckhaus boundaries from the low-velocity regime until the planar-front restabilization. We pay a special attention to the experiments on liquid crystals [J. M. Flesselles, A. J. Simon, and A. J. Libchaber, Adv. Phys. **40**, 1 (1991)]. The special shape of the Eckhaus boundaries in the present situation provides a simple hint for experimental investigations. The second line of this paper is motivated by a strong wish to go further towards the understanding of the diverse variety of dynamical manifestations observed in experiments, such as oscillatory modes and "chaotic" motions. The study of these phenomena is greatly facilitated by focusing on the large-velocity regime where the front dynamics turns out to be described by a local equation. We outline here the derivation of that equation appropriate for liquid-crystal experiments. A full study on this equation, going from order to chaos, is presented elsewhere [K. Kassner, C. Misbah, and H. Müller-Krumbhaar, Phys. Rev. Lett. **67**, 1551 (1991)]. Among other results presented here we show that the wavelength of the pattern λ scales with the growth velocity V and the thermal gradient as $\lambda \sim V^{-1} f(G/V)$. At the fold singularity for steady symmetric solutions, we find that $\lambda \sim V^{-1}$, which is in agreement with experiments on liquid crystals. This scaling is to be contrasted to the one obtained in the small-Péclet-number limit $\lambda \sim V^{-1/2} f(G/V)$ [K. Kassner and C. Misbah, Phys. Rev. Lett. **66**, 445 (1991)].

PACS number(s): 61.50.Cj, 05.70.Fh, 81.30.Fb, 68.70.+w

I. INTRODUCTION

When a dilute binary solid grows by directional solidification at the expense of its melt, the planar liquid-solid interface undergoes a morphological instability at a critical growth speed and develops a cellular structure [1]. The front instability was first analyzed by Mullins and Sekerka [2]. They were the first to bring out the kinetic nature of the phenomenon. Since then, extensive experimental and theoretical investigations have been devoted to pattern formation in directional solidification [1].

We feel it worthwhile to emphasize the major difference that exists between a system where mass diffusion is one-sided, and a system where mass diffusion is symmetric (or at least of comparable importance in both phases). The first category includes metals and some organic compounds [3] with diffusion coefficient in the solid phase several orders of magnitude smaller than in the liquid phase. In that category one often observes the development of large-amplitude cells with accumulation of solute in the groove. The creation of deep grooves often causes the appearance of crystal defects, such as, for instance, grain boundaries, which are rather secondary for the understanding of interface dynamics. The second category is mainly restricted to liquid-crystal systems where experiments were initiated by Oswald, Bechhoefer, and Libchaber [4]. The quasisymmetric impurity diffusion with the quasiconstant miscibility gap makes the dynamics much softer than in the first category, in the sense that nonlinearities are less important and that deep grooves never develop. Such systems have allowed the exploration of a much larger region of the parameter space than what usual materials had allowed us so far, and have led to the discovery of a myriad of dynamical phenomena.

A step in understanding interface shapes in the highly nonlinear regime came from numerical solution of steady periodic interfaces [5] and from a forward-time-dependent calculation [6,7]. These calculations are performed with finite sizes (often with one to two wavelengths) and therefore do not allow for the competition between the active modes in the admissible continuum. This restriction may be important since there is experimental evidence for a variety of free boundary systems that soft instabilities of phase type play an important role in the process by which new patterns are selected [8].

Assume that $\zeta_0(qx)$ represents a one-dimensional steady-state periodic solution of the growth equation with wavelength $2\pi/q$, $\zeta_0(qx+\varphi)$ with φ a constant, is also a solution for an extended system. For an infinitesimal phase shift, $\varphi \ll 1$, one has $\zeta_0(qx+\varphi) \simeq \zeta_0(qx) + (\varphi/q)(\partial\zeta_0/\partial x)$, where $\partial\zeta_0/\partial x$ is the Goldstone mode which is a neutral mode of the linearized operator. It is therefore natural to expect large-wavelength phase fluctuations to be dangerous. Our first aim is to present an

extensive study of the phase dynamics by adopting a nonlinear WKB method in the boundary integral formulation. Although our analysis will work perfectly well in any general situation, we will confine ourselves here to the experimental setup of Simon, Bechhoefer, and Libchaber [8]. Since it has been possible to explore experimentally the whole bifurcation curve predicted by Mullins and Sekerka [2], until the planar-front restabilization, we will compute the boundaries of phase instability (Eckhaus instability) in the whole range inside the tongue where the planar front is unstable. As expected [9], we find that the actual Eckhaus band is, even close to the threshold for the planar-front instability, significantly different from that obtained from the lowest-order amplitude theory. It will emerge from our analysis that the band of allowed states is significantly reduced but it is still finite so that we are still faced with the longstanding puzzle of wavelength selection. Another important result to emerge here is that the Eckhaus tongue in the "wavenumber–velocity" plane is strongly tilted, so that it offers a simple way for the experimental study of the Eckhaus instability. Indeed, the experimental protocol naturally suggested by this consists in sudden jumps in the pulling speed.

Of course the phase instability is not the only important dynamical manifestation. Recently directional solidification of liquid crystals and other one-dimensional pattern-forming systems have exhibited a variety of symmetry-breaking instabilities. A particularly interesting mode is the so-called solitary asymmetric mode that travels sideways and seems to play a wavelength-selector role [10]. This phenomenon is common to other one-dimensional systems such as lamellar eutectics [11] and fluid-fluid systems in the printer geometry [12]. It has now been well established phenomenologically [13] and by solving the "microscopic" equations [14] that this dynamical manifestation results from a secondary bifurcation of the underlying symmetric state. Another common mode is the optical mode where the cell width oscillates in phase opposition with its neighbors [10]. When the system is driven far away from the point where these structures take place, the interface seems to develop an "erratic" motion that was tentatively called "chaos" [10]. In general, dealing with these complex dynamics would mean solving the full boundary integral equation. This equation involves nonlocal and retarded interactions which prove difficult to elucidate in both analytical and numerical investigations.

By realizing that in the Simon, Bechhoefer, and Libchaber [8] experiment most of the above-mentioned dynamical manifestations occur in a regime where the wavelength of the pattern is much larger than the diffusion length, we could expect the dynamics to be quasilocal. By using a singular expansion first devised by Sivashinsky [15] and adopted by Brattkus and Davis [16] for the one-sided model, we derive here from the full growth equations the only part that is relevant to the front dynamics for liquid crystals in the regime of interest. This is a nonlinear partial differential equation which is much more tractable than the integral equation and, despite its simplicity, exhibits a large variety of dynamical patterns going from order to chaos [17]. The discovery of vacillating-breathing mode (or optical mode) and a generic route to the transition into chaos were presented recently [17]. Our main objective here is to give the derivation of the local equation and to emphasize the great progress offered by this equation in understanding the various complex dynamics. We will also discuss some other aspects related to the scaling of the wavelength of the pattern in this regime and compare our results to experimental findings.

This paper is organized as follows. In Sec. II we write down the basic equations of growth which are relevant to liquid-crystal experiments. We then convert them into a boundary integral equation. In Sec. III we take the integral equation as a starting point, we extract from it only that part which is relevant to phase motion, and we evaluate it analytically in the vicinity of the Mullins-Sekerka instability. Section IV is devoted to the general calculation of the phase equation at an arbitrary distance from the threshold. This involves a numerical solution of the steady-interface profile and the adjoint function to the deviation from the steady profile. Section V contains the results for the phase instability and their discussion. In Sec. VI we give a derivation of the local equation that is valid at large enough growth speeds and discuss some aspects of the results. Some concluding remarks are presented in Sec. VII.

II. BASIC EQUATIONS

We consider the following situation: an impure nematic crystal is grown in the z direction at the expense of its isotropic phase by translating the sample at a constant velocity V across a thermal gradient G established via a "hot" and a "cold" contact (Fig. 1). The concentration of impurities far ahead of the advancing interface is denoted by c_∞. The diffusion coefficient of impurities in the crystalline phase is of the same order of magnitude as in the isotropic phase. We will assume here that this diffusion is symmetric. Let $u=(c-c_\infty)/\Delta c$ denote the dimensionless concentration field in both phases, where $\Delta c=c_\infty(1-k)/k$ is the equilibrium concentration gap

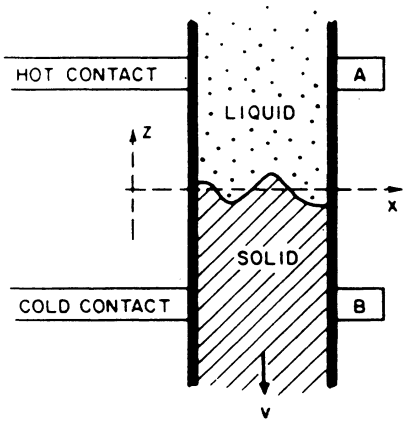

FIG. 1. A schematic plot of the directional-solidification setup.

and k the partition coefficient. We consider one-dimensional deformations only and assume that the system is infinite in the x direction (on the scale of all wavelengths of interest). Mass conservation in the bulk, expressed in the laboratory frame, takes the form

$$\frac{\partial u}{\partial t}=2\frac{\partial u}{\partial z}+\nabla^2 u \ , \tag{1}$$

where lengths and time are measured in $l=2D/V$ and l^2/D units, respectively. l is the diffusion length, and D the diffusion constant. At the liquid-crystal interface, the continuity and the Gibbs-Thomson conditions read, respectively,

$$\frac{\partial u_s}{\partial n}-\frac{\partial u_l}{\partial n}=(2+\dot{\zeta})n_z[k+(1-k)u_l] \ , \tag{2}$$

$$u_l=1-d_0\kappa-\frac{\zeta}{l_T} \ , \tag{3}$$

where the subscripts l and s refer to the liquid and the crystalline phase, respectively, $\partial/\partial n$ stands for the normal derivative,

$$d_0=\frac{\gamma T_M}{mlL\Delta c} \ , \quad l_T=\frac{m\Delta c}{lG} \tag{4}$$

are the reduced capillary length and the thermal length, respectively, where γ is the surface tension, T_M the melting temperature of the pure substance, m the absolute value of the liquidus slope, L the latent heat of fusion per unit volume, and G the applied thermal gradient. Finally κ is the curvature taken to be positive for a convex crystal

$$\kappa=-\frac{\zeta_{xx}}{(1+\zeta_x^2)^{3/2}} \ . \tag{5}$$

Note that in writing Eq. (2) we have made use of the relation $c_s=kc_l$. In terms of our dimensionless quantities, this equation transforms into

$$u_s=k(u_l-1) \ . \tag{6}$$

Note also that Eq. (3) assumes that there is no dissipation at the interface and that the thermal profile is constant throughout the sample. This is justified provided that the heat diffusion plays no role and that the thermal properties of both phases are identical. The latter situation can be achieved by using highly conducting plates so that the heat diffuses essentially through them rather than through the sample itself, while the first assumption is usually satisfied because the temperature profile is adiabatically slaved to the concentration profile. Finally, since c_l is maintained at a constant value at distances much larger than the diffusion length, the condition on u_l far ahead of the front amounts for all practical purposes to

$$u_l(z\to\infty)=0 \ . \tag{7}$$

Equations (1)–(3) and (7) completely describe the dynamics of solidification. For the experimental setup of Simon, Bechhoefer, and Libchaber [8] $k\simeq 0.9$. In what follows we will assume a constant miscibility gap, namely, $k=1$. This will substantially simplify the algebra. It is possible, by using the Green's-function techniques to convert this set of equations into a closed integral equation for the front profile. The method is standard, we simply give the result [18]

$$1-d_0\kappa-\frac{\zeta}{l_T}=\int_{-\infty}^{\infty}dt'\int_{-\infty}^{\infty}dx'(2+\dot{\zeta})\mathcal{G}(x,\zeta(x,t),t|x',\zeta(x',t'),t') \ , \tag{8}$$

where

$$\mathcal{G}=\frac{\Theta(\Delta t)}{4\pi\Delta t}\exp\left[-\frac{\Delta x^2+\Delta\zeta^2+(\Delta\zeta+2\Delta t)^2}{4\Delta t}\right] \tag{9}$$

is the diffusion propagator, Θ is the Heaviside step function, and $\Delta x=x-x'$, $\Delta t=t-t'$, $\Delta\zeta=\zeta(x,t)-\zeta(x',t')$. Equation (8) constitutes our starting point for the derivation of the phase-diffusion equation.

III. DERIVATION OF THE PHASE-DIFFUSION EQUATION

Although our derivation can be made more general than presented here, as can be recognized in our treatment below, we will consider the quasistationary approximation. This approximation correctly identifies the Eckhaus boundaries, and since our purpose is to determine these boundaries, then this is largely sufficient. The quasistationary assumption means that we can replace in the kernel of the integral equation $\zeta(x',t')$ by $\zeta(x',t)$. Therefore the only dependence on t' that remains in the integrand comes from Δt. We can thus perform the integration over t', so that Eq. (8) becomes

$$1-d_0\kappa-\frac{\zeta}{l_T}=\frac{1}{2\pi}\int_{-\infty}^{\infty}dx'(2+\dot{\zeta})\exp(-\Delta\zeta)\times K_0((\Delta\zeta^2+\Delta x^2)^{1/2}) \ , \tag{10}$$

where K_0 is the modified Bessel function of order zero.

To derive the phase equation, we adopt a nonlinear WKB method such as that used by Kramer *et al.* [19] in the framework of reaction-diffusion equations. This method is popular in the nonlinear oscillator community [20]. The first step of the method consists in seeking solutions which are 2π periodic in a certain phase $\varphi(x,t)$

to be defined below. In a completely homogeneous system $\varphi = q_0 x$, q_0 being a constant wave number characterizing the periodic structure. In the presence of wavelength fluctuations, however, the wave number is no longer constant but varies in space and eventually in time. Since we are interested in slowly varying modulations, the local wave number is a slow function of x and t. The demand that the wave number q is a slow function of space is satisfied by requiring that $\varphi(x,t)$ scales as $\varphi \sim \Phi(X,t)/\epsilon$, where ϵ is an auxiliary small parameter measuring the strength of the modulation, and ϕ a slow function of space as explicitly expressed by the introduction of the slow variable $X \equiv \epsilon x$. On the other hand, because we are interested in a diffusion process, we may expect the characteristic time scale of motion of interest to be of order ϵ^{-2}. We therefore introduce the slow time variable $\tau \equiv \epsilon^2 t$ and write the rapid phase as

$$\varphi = \frac{\phi(X,\tau)}{\epsilon} . \tag{11}$$

We then write formally $\zeta(x,t) = \zeta(\varphi,X,\tau)$ as if it were depending separately on the rapid variable φ and the slow variables X and τ. We are therefore to understand that we must make the substitutions

$$\frac{\partial}{\partial x} \to q\frac{\partial}{\partial \varphi} + \epsilon\frac{\partial}{\partial X} , \quad \frac{\partial}{\partial t} \to \epsilon\frac{\partial \phi}{\partial \tau}\frac{\partial}{\partial \varphi} + \epsilon^2\frac{\partial}{\partial \tau} \tag{12}$$

whenever we differentiate ζ with respect to x and to t, respectively; $q = \partial\phi/\partial X$ is the local wave number. Now the scheme is to expand ζ in power series of ϵ:

$$\zeta = \zeta_0(\varphi,X,\tau) + \epsilon\zeta_1(\varphi,X,\tau) + \cdots . \tag{13}$$

If our Eq. (10) were local, we could then have to insert Eqs. (12) and (13) into that equation and deduce in a systematic way successively higher-order contributions in ϵ. The present situation is, however, less trivial than with ordinary partial differential equations. Here, in addition to the systematic multiscale analysis to be used for the differential operators, one has to express too the slow modulations in the kernel of the integral equation. This situation is similar in principle to that used, for example, in superconductivity when one performs the Landau-Ginzburg limit from the BCS theory [21].

Using the fact that the differential of the integration variable x' is related to the phase φ' by $dx' = d\varphi'/q(\varphi')$ and expanding $q(\varphi')$ about $\varphi' = \varphi$, we obtain to order ϵ

$$dx' = \frac{d\varphi'}{q(\varphi)}\left[1 - \epsilon\frac{(\varphi'-\varphi)}{q^2(\varphi)}\frac{\partial q}{\partial X}\right] , \tag{14}$$

and in a similar way

$$\Delta x = \frac{\varphi-\varphi'}{q} + \epsilon\frac{(\varphi'-\varphi)^2}{2q^3}\frac{\partial q}{\partial X} . \tag{15}$$

The time derivative $\dot{\zeta}$ that appears in Eq. (10) reads

$$\dot{\zeta} = \epsilon\frac{\partial \zeta_0(\varphi,X)}{\partial \varphi}\frac{\partial \phi}{\partial \tau} . \tag{16}$$

We still need to write $\Delta\zeta$ in Eq. (10) in terms of the variables φ, φ', X and τ. To do so, we first write $\Delta\zeta$ by displaying its arguments:

$$\Delta\zeta = \zeta(\varphi,X,\tau) - \zeta(\varphi',X',\tau') . \tag{17}$$

We then replace ζ by its expansion [Eq. (13)]:

$$\Delta\zeta = \zeta(\varphi,X,\tau) - \zeta_0(\varphi',X',\tau') + \epsilon[\zeta_1(\varphi,X,\tau) - \zeta_1(\varphi',X',\tau')] + O(\epsilon^2) . \tag{18}$$

Since ζ_1 multiplies ϵ, the slow arguments X' and τ' in ζ_1 can be set equal to X and τ, respectively, since their variations induce higher-order contributions in ϵ. For the ζ_0 terms, we expand $\zeta_0(\varphi',X',\tau')$ about $X' = X$ for the space modulations, while the temporal ones are of order ϵ^2 and can be ignored. In other words,

$$\zeta_0(\varphi',X',\tau') = \zeta_0(\varphi',X,\tau) + \epsilon\frac{(\varphi'-\varphi)}{q(\varphi)}\frac{\partial \zeta_0(\varphi,X,\tau)}{\partial X} + O(\epsilon^2) . \tag{19}$$

Inserting Eq. (19) into Eq. (18) and taking into account the above-mentioned remarks, we obtain

$$\Delta\zeta = \zeta_0(\varphi,X,\tau) - \zeta_0(\varphi',X,\tau) - \epsilon\frac{(\varphi'-\varphi)}{q(\varphi)}\frac{\partial \zeta_0(\varphi,X,\tau)}{\partial X} + \epsilon[\zeta_1(\varphi,X,\tau) - \zeta_1(\varphi',X,\tau)] + O(\epsilon^2) . \tag{20}$$

From now on, since all the dependences on the slow variables contain X and τ (and not X' and τ'), we will omit these arguments. Having this in mind, we will now plug Eqs. (16) and (20) into Eq. (10) and classify the contributions order by order.

A. Order ϵ^0

To this order we obtain

$$1 - d_0\kappa_0 - \frac{\zeta_0}{l_T} = \frac{1}{\pi q}\int_{-\infty}^{\infty} d\varphi' \exp(-\Delta\zeta_0)K_0(\rho_0) , \tag{21}$$

where the curvature κ_0 is given by

$$\kappa_0 = -\frac{q^2\dfrac{\partial^2\zeta_0}{\partial\varphi^2}}{\left[1 + \left[\dfrac{\partial\zeta_0}{\partial\varphi}\right]^2\right]^{3/2}} , \tag{22}$$

$\Delta\zeta_0 \equiv \zeta_0(\varphi) - \zeta_0(\varphi')$, $\rho_0 \equiv [(\Delta\varphi q)^2 + \Delta\zeta_0^2]^{1/2}$, $\Delta\varphi \equiv \varphi - \varphi'$, and K_0 is the modified Bessel function of order zero.

Equation (21) represents the steady version of the full integral equation (10) parametrized by the local wave number $q(X,\tau)$.

B. Order ϵ

To this order we obtain an inhomogeneous equation for ζ_1,

$$L\zeta_1 = f \ , \tag{23}$$

where L is the Fréchet derivative of the integral equation with respect to ζ, evaluated at ζ_0. It is given by

$$L\zeta_1 = d_0 q^2 \frac{\partial}{\partial\varphi}\left[\mathcal{D}_0^{-3/2}\frac{\partial}{\partial\varphi}\zeta_1\right] - \frac{\zeta_1}{l_T} + \frac{1}{\pi}\int_{-\infty}^{\infty}\frac{d\varphi'}{q}\exp(-\Delta\zeta_0) \times\left[K_0(\rho_0)+\frac{\Delta\zeta_0}{\rho_0}K_1(\rho_0)\right]\Delta\zeta_1 \ , \tag{24}$$

where K_1 is the modified Bessel function of order one, and $\mathcal{D}_0 \equiv (1+q^2\partial^2\zeta_0/\partial\varphi^2)^{-1}$. The homogeneous part in Eq. (23) which arises from phase modulations takes the form

$$f = \frac{1}{2\pi q}\frac{\partial\phi}{\partial\tau}\int_{-\infty}^{\infty}d\varphi'\frac{\partial\zeta_0}{\partial\varphi'}\exp(-\Delta\zeta_0)K_0(\rho_0) - \frac{\partial^2\phi}{\partial X^2}d_0\left\{\left[2q\frac{\partial^2\zeta_0}{\partial\varphi\partial q}+\frac{\partial\zeta_0}{\partial\varphi}\right]\mathcal{D}_0^{-3/2} - 3q^2\frac{\partial\zeta_0}{\partial\varphi}\frac{\partial^2\zeta_0}{\partial\varphi^2}\frac{\partial\zeta_0}{\partial q}\mathcal{D}_0^{-5/2}\right\}$$
$$-\frac{1}{\pi q^2}\frac{\partial^2\phi}{\partial X^2}\int_{-\infty}^{\infty}d\varphi'\Delta\varphi\exp(-\Delta\zeta_0)\left\{\left[\frac{\partial\zeta_0}{\partial q}-\frac{1}{q}\right]K_0(\rho_0)+\left[\frac{\Delta\varphi^2}{2q^3}+\frac{\partial\zeta_0}{\partial q}\Delta\zeta_0\right]\frac{K_1}{\rho_0}\right\} . \tag{25}$$

In writing this expression we have made use of the fact that ζ_0 depends on the slow variable X only via $q(X,\tau)$ and that therefore we can write $\partial\zeta_0/\partial X = (\partial q/\partial X)\partial\zeta_0/\partial q = (\partial^2\phi/\partial X^2)\partial\zeta_0/\partial q$. It is easily shown that the linear operator L has the translational solution $\partial\zeta_0/\partial\varphi$. It follows from the Fredholm alternative theorem that the adjoint operator $L^\dagger$ has a nontrivial null space and that ζ_1 exists only if the inhomogeneous term is orthogonal to the null space. This solvability condition leads to the sought after phase-diffusion equation. For this purpose we first rewrite Eq. (23) by using the definition of the linear operator L in Eq. (24) as

$$d_0 q^2\frac{\partial}{\partial\varphi}\left[\mathcal{D}_0^{-3/2}\frac{\partial}{\partial\varphi}\zeta_1\right] - \frac{\zeta_1}{l_T} + \int_{-\infty}^{\infty}d\varphi'\mathcal{A}(\varphi,\varphi')\Delta\zeta_1 = f \ , \tag{26}$$

where we have introduced the abbreviation $\mathcal{A}(\varphi,\varphi')$ for the kernel which is defined by

$$\mathcal{A}(\varphi,\varphi') = \frac{1}{\pi q}\left[K_0(\rho_0)+\frac{\Delta\zeta_0}{\rho_0}K_1(\rho_0)\right]\exp(-\Delta\zeta_0) \ , \tag{27}$$

which depends on the zeroth-order solution only. The procedure now consists of multiplying Eq. (26) by the adjoint function $\zeta_1^\dagger(\varphi)$ which is taken to be 2π periodic, and integrating over one period

$$\int_0^{2\pi}d\varphi\left[d_0 q^2\frac{\partial}{\partial\varphi}\left[\mathcal{D}_0^{-3/2}\frac{\partial}{\partial\varphi}\zeta_1\right]-\frac{\zeta_1}{l_T}\right]\zeta_1^\dagger(\varphi)$$
$$+\sum_m\int_0^{2\pi}d\varphi\int_0^{2\pi}d\varphi'\mathcal{A}(\varphi,\varphi'+2\pi m)[\zeta_1(\varphi)-\zeta_1(\varphi')]\zeta_1^\dagger(\varphi) = \int_0^{2\pi}d\varphi f(\varphi)\zeta_1^\dagger(\varphi) \ , \tag{28}$$

where we have restricted the integration over φ' in the original integral term in the interval $(0,2\pi)$ for reasons that will become clear below. The operator that appears in the integrand of the first integral is self-adjoint (this is the Liouville operator); we can therefore interchange ζ_1 and $\zeta_1^\dagger$. In the second integral, we split it in two parts, one containing $\zeta_1(\varphi)\zeta_1^\dagger(\varphi)$ and the other containing $\zeta_1(\varphi')\zeta_1^\dagger(\varphi)$. We are to understand here that since $\mathcal{A}$ contains a Cauchy singularity, each of the two parts should be taken in the Cauchy principal value sense. The part that contains $\zeta_1(\varphi)\zeta_1^\dagger(\varphi)$ is obviously self-adjoint, while this is not the case for the part containing $\zeta_1(\varphi')\zeta_1^\dagger(\varphi)$, since the kernel $\mathcal{A}$ is not symmetric under the permutation of φ and φ'. Since the integration variables φ and φ' are dummy variables and each of them is confined to the same interval, we can interchange φ and φ'. After all these manipulations we obtain

$$\int_0^{2\pi} d\varphi \left[d_0 q^2 \frac{\partial}{\partial \varphi}(\mathcal{D}_0^{-3/2}\zeta_1^\dagger) - \frac{\zeta_1^\dagger}{l_T} \right] \zeta_1(\varphi) + \int_0^{2\pi} d\varphi \zeta_1(\varphi) \left[\zeta_1^\dagger(\varphi) \mathcal{P} \int_{-\infty}^{\infty} \mathcal{A}(\varphi,\varphi') d\varphi' - \mathcal{P} \int_{-\infty}^{\infty} \mathcal{A}(\varphi',\varphi) \zeta_1^\dagger(\varphi') d\varphi' \right] = \int_0^{2\pi} d\varphi \zeta_1^\dagger f \ , \quad (29)$$

where $\mathcal{P}$ stands for Cauchy principal value.

To define the adjoint homogeneous problem, we consider the homogeneous problem ($f=0$). Then the equations should be satisfied for arbitrary but small deviations ζ_1 about ζ_0. This entails that the adjoint function $\zeta_1^\dagger$ should satisfy

$$L^\dagger \zeta_1^\dagger \equiv d_0 q^2 \frac{\partial}{\partial \varphi}(\mathcal{D}_0^{-3/2}\zeta_1^\dagger) - \frac{\zeta_1^\dagger}{l_T} + \zeta_1^\dagger \mathcal{P} \int_{-\infty}^{\infty} \mathcal{A}(\varphi,\varphi') d\varphi' - \mathcal{P} \int_{-\infty}^{\infty} \mathcal{A}(\varphi',\varphi) \zeta_1^\dagger(\varphi') d\varphi = 0 \ . \quad (30)$$

Having defined the adjoint problem in this way, we immediately obtain from Eq. (29) the solvability condition $\int_0^{2\pi} d\varphi \zeta_1^\dagger f = 0$ which results in the sought after phase-diffusion equation

$$\frac{\partial \phi}{\partial \tau} = \Lambda \frac{\partial^2 \phi}{\partial X^2} \quad (31)$$

where $\Lambda(q)$ is the phase-diffusion coefficient defined by

$$\frac{\Lambda(q)}{2\pi q} \int_0^{2\pi} d\varphi' \int_{-\infty}^{\infty} d\varphi \frac{\partial \zeta_0}{\partial \varphi} \exp(-\Delta\zeta_0) K_0(\rho_0) \zeta_1^\dagger(\varphi)$$
$$= \int_0^{2\pi} d\varphi \, d_0 \left\{ \left[2q \frac{\partial^2 \zeta_0}{\partial \varphi \partial q} + \frac{\partial \zeta_0}{\partial \varphi} \right] \mathcal{D}_0^{-3/2} - 3q^3 \frac{\partial \zeta_0}{\partial \varphi} \frac{\partial^2 \zeta_0}{\partial \varphi^2} \frac{\partial \zeta_0}{\partial q} \mathcal{D}_0^{-5/2} \right\} \zeta_1^\dagger$$
$$+ \frac{1}{\pi q^2} \int_0^{2\pi} d\varphi' \int_{-\infty}^{\infty} d\varphi \, \Delta\varphi \exp(-\Delta\zeta_0) \left\{ \left[\frac{\partial \zeta_0}{\partial q} - \frac{1}{q} \right] K_0(\rho_0) + \left[\frac{\Delta\varphi^2}{2q^3} + \frac{\partial \zeta_0}{\partial q} \Delta\zeta_0 \right] \frac{K_1(\rho_0)}{\rho_0} \right\} \zeta_1^\dagger \ . \quad (32)$$

Equation (31) constitutes a general phase-diffusion equation which is valid at arbitrary distance above the Mullins-Sekerka threshold. The evaluation of the phase-diffusion coefficient $\Lambda(q)$ requires the determination of both the steady-state solution $\zeta_0(\varphi)$ which satisfies Eq. (21), and the adjoint function $\zeta_1^\dagger(\varphi)$ which obeys Eq. (30). Far away from the threshold, these quantities can only be determined numerically. Close to the threshold, however, an analytic evaluation is possible by means of an amplitude expansion. To leading order in a standard amplitude expansion, the stationary profile ζ_0 can be written as

$$\zeta_0 \simeq \sqrt{\nu} \left[1 - \frac{\beta_0}{\sqrt{\nu}} (q - q_c)^2 \right]^{1/2} \cos\varphi \ , \quad (33)$$

where $\beta_0 = \frac{1}{2} \partial^2 \omega / \partial q^2 |_{q=q_c}$, with ω the Mullins-Sekerka growth rate, q_c the critical wave number, and ν a small parameter measuring the distance from threshold and defined in such a way that $\epsilon = \beta_0 (q - q_c)^2$ is, to lowest order, the neutral curve. To leading order in ν, it is easy to see that the kernel $\mathcal{A}(\varphi,\varphi')$ defined by Eq. (27) is symmetric in φ and φ' since $\Delta\zeta_0 \simeq 0$ and ρ_0 is symmetric. This means that the linear operator is self-adjoint in this limit. It then follows that $L^\dagger \zeta_1^\dagger = 0$ is solved by the Goldstone mode

$$\zeta_1^\dagger \sim \frac{\partial \zeta_0}{\partial \varphi} \sim \sin\varphi \quad (34)$$

up to an arbitrary multiplicative constant. Substituting Eqs. (33) and (34) into Eq. (32), we obtain to leading order in an expansion in $\sqrt{\nu}$ and $(q - q_c)$ that the phase-diffusion constant is given by

$$\Lambda(q) = \frac{1 - 3\beta_0 (q - q_c)^2 / \nu}{1 - \beta_0 (q - q_c)^2 / \nu} \ . \quad (35)$$

This expresses the well-known Eckhaus result [22], which is quite general close to the threshold, since there the front dynamics is always described by the complex Landau-Ginzburg equation. This equation is universal in the sense that its form does not depend on the physical details but on symmetry properties only. Equation (35) indicates that modes with wave numbers q such that

$$|q - q_c| > \left[\frac{\nu}{3\beta_0} \right]^{1/2} \quad (36)$$

are unstable against long-wavelength phase fluctuations. Since the neutral curve is defined by $|q - q_c| = (\nu/\beta_0)^{1/2}$, Eq. (36) shows that the phase instability reduces the band of linearly unstable modes by a factor $\sqrt{3}$. We are therefore left with a finite stable band.

The phase band given by the Eckhaus result has been studied in Rayleigh-Bénard convection and seems to represent well the phase instability boundaries even far enough from the threshold. While the amplitude theory describes well the Eckhaus instability in Rayleigh-Bénard convection, this is not the case, however, for the Taylor-Couette system [23], where a significant deviation from

the full calculation was found. Also there was a strong suspicion for the directional-solidification systems that the result (35) should not be accurate even very close to the threshold. The reason is the mixing of two disparate length scales, the diffusion length (usually of the order of 100 μm) and the capillary length (of the atomic scale). The result is a broad spectrum of marginal modes near the threshold that causes a vigorous mode mixing which usually escapes standard perturbative techniques. One therefore naturally expects the lowest-order expansions to be inadequate. That was the major motive for the derivation of a general phase equation. As we demonstrated in a previous Letter [9], and we shall see below, there is, as expected, a strong deviation of the actual Eckhaus boundary from that expressed by Eq. (35).

IV. NUMERICAL METHOD

In order to determine the Eckhaus boundaries at an arbitrary distance from the Mullins-Sekerka threshold we have evaluated the diffusion constant numerically. As can be seen from Eq. (32), this evaluation requires the determination of both the stationary profile ζ_0, which obeys Eq. (21), and the adjoint function $\zeta_1^\dagger$ which belongs to the kernel of the adjoint operator $L^\dagger$ [see Eq. (30)]. The method for solving for ζ_0 is by now standard and we will therefore keep the discussion brief and merely emphasize the strategy. An extensive discussion of the method has been given recently in the context of eutectic growth [24]. Our method of discretization of the interface is the boundary element method [25], which has been used by Saito, Golbeck-Wood and Müller-Krumbhaar [26] in the context of free dendritic growth. We find it convenient to represent the interface by its intrinsic coordinates rather than by Cartesian coordinates. That is, we take the angle $\theta(s)$ between the normal to the interface and the growth axis as a function of the curvilinear coordinate s as the unknown. We consider symmetric and periodic solutions so that the integration interval can be taken to be $(0,\lambda/2)$. If N is the number of discretization points over this interval, we have $N-1$ angles θ_i (we take all the points to be equidistant). An intrinsic representation has, by its very nature, an arbitrary origin. The translational invariance tells us that the x coordinate of that origin can be taken anywhere (here we choose it at $x=0$). However, because of the existence of an external thermal gradient, the z coordinate of that origin is not arbitrary but should be fixed self-consistently. Let this unknown be denoted by z_0. We then have N variables in total $(\theta_1,\ldots,\theta_{N-1},z_0)$. We have N equations in turn. Indeed we impose the integral equation [Eq. (21)] everywhere except at the end points of the integration domain, which means that we solve that equation for $N-2$ points. At the two end points (0 and $\lambda/2$) we impose the smoothness condition instead. That is, we impose that $\zeta'(0)=0$ and $\zeta'(\lambda/2)=0$. The total number of equations is N also, and the problem is well posed. After discretization we obtain N nonlinear algebraic equations for the N unknowns. These equations are solved by means of a standard Newton-Raphson scheme. There is, however, one complication: we cannot prevent the Newton-Raphson method from converging to the planar-front solution, which exists everywhere in the parameter space. We can circumvent this difficulty by using the following trick. We force temporarily the interface position at $x=0$ to a prescribed value z_0. By doing so we cannot in general satisfy the smoothness condition at $x=0$, unless we miraculously choose the exact value for z_0. This means that in general the interface shape will exhibit cusps at $x=0$. We will then progressively vary z_0 until the condition $\zeta'(0)=0$ is met. This happens for isolated values of z_0 (but λ is arbitrary inside the neutral curve). Once a nonplanar and physical solution is found, we can vary progressively the parameters (e.g., $\lambda, V,\ldots$) in a certain desired direction and follow the evolution of the front profile.

Figure 2 shows a typical front profile. We should remark, in accord with what we mentioned in the introduction, that the interface never develops deep grooves; the front deformation is of the order of the wavelength. The reason for this behavior is twofold. (i) The partition coefficient in the liquid-crystal system is close to one. As a consequence the band of unstable modes is significantly smaller [7] than the one met in ordinary systems (e.g., succinonitrile). (ii) The impurity diffusion is quasisymmetric. There exists now in the crystalline phase a short circuit of the mass current that operates on the scale of the wavelength, which thereby strongly reduces the development of the front deformation.

The next step of our investigation consists in solving for the adjoint function $\zeta_1^\dagger$ which satisfies the equation $\mathcal{L}^\dagger\zeta_1^\dagger=0$. This equation is linear and nonlocal. The method of discretization is similar to the one used above for the steady-state problem. The logarithmic and the algebraic singularities arising from the Bessel functions K_0 and K_1 are extracted analytically. The equation for $\zeta_1^\dagger$ can be formally written in a matrix form

$$BX^\dagger=0\ , \tag{37}$$

where the matrix B depends on the zeroth-order solution ζ_0, and $X^\dagger$ is a column vector representing $\zeta_1^\dagger$. If Eq. (37) is to have a nontrivial solution, the matrix B should be singular. The problem amounts then to searching for those nonzero $X^\dagger$ elements which satisfy Eq. (37). To find the null space of B we have made use of the singular-value decomposition method [27]. The method consists in decomposing B as

$$B=UMV^T\ , \tag{38}$$

where U and V are orthogonal matrices ($UU^T=1$ and

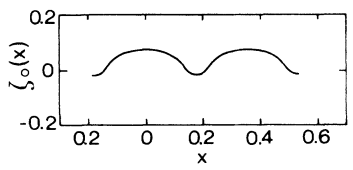

FIG. 2. A typical front profile.

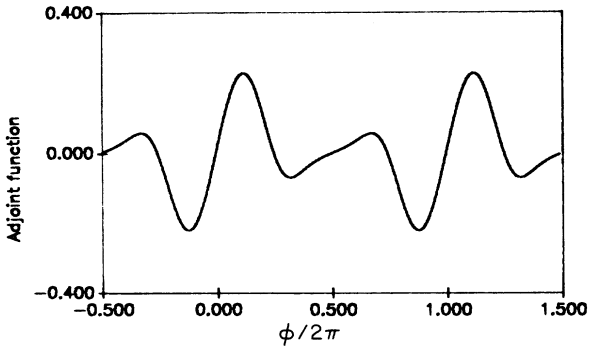

FIG. 3. A typical form of the adjoint function.

$VV^T=1$) and M is a diagonal matrix whose (nonnegative) elements ω_i are called the singular values of B. Equation (38) can be thought of as a generalization of the diagonalization theorem to an arbitrary matrix. If B is a singular matrix, this means that the (diagonal) matrix M has at least one singular value which is zero. The number of the zero singular values defines the nullity of B. The nontrivial elements $X^\dagger$ are given by the column vectors of V whose same numbered elements ω_i are zero. It goes without saying that the computed singular values can be expected at best to be as precise as the computed solution ζ_0 (approximately 10^{-3}). Very close to the Mullins-Sekerka threshold ($\ll 1\%$) we find two singular values of size 10^{-4} and 10^{-3} while the others are significantly larger (>0.1). One of the singular eigenfunctions is the antisymmetric translational solution and the other is a symmetric shadow of the linearized cell. Slightly above the threshold only the singular value of the antisymmetric solution remains small and the corresponding eigenfunction quickly deviates from the translational mode. Figure 3 shows a typical eigenfunction.

V. THE RESULTS

Having determined the stationary profile ζ_0 and the adjoint function $\zeta_1^\dagger$, we are in a position to determine the Eckhaus boundaries. These are determined by the condition that the diffusion coefficient $\Lambda(q)$ vanishes. Close to the Mullins-Sekerka threshold we use the result which follows from the amplitude theory to guess both the profile ζ_0 and the Eckhaus boundary. Once a point on the Eckhaus boundary is determined, we use successive extrapolations to determine the guess for next points and so on. The overall picture of our results is summarized in Figs. 4 and 5. There we have chosen our units so that the impurity diffusion constant D and the physical thermal length are both equal to one. In these units we have taken $d_0=10^{-2}$, which is a typical value in liquid-crystal systems [10]. Figure 4 shows our results close to the Mullins-Sekerka threshold, and their comparison to the usual amplitude theory. The full line represents the neutral curve, the dashed line the Eckhaus boundaries obtained from the amplitude equation, the symbols the Eckhaus boundaries determined from the full calculation, and the dotted curve the linearly most dangerous mode.

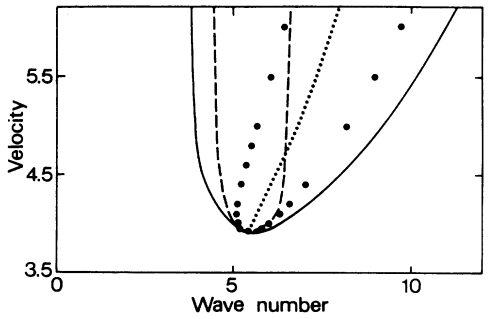

FIG. 4. The full line represents the neutral curve, the dashed line the Eckhaus boundaries computed from the lowest-order amplitude equation, the symbols the actual Eckhaus boundaries, the dotted line the linearly most dangerous mode. These results are computed close to the Mullins-Sekerka threshold.

The deviation of our result from those which follow from the amplitude theory is dramatic. This result clearly indicates that, despite the moderate deformation of the interface, the front dynamics strongly escape the standard amplitude description even very close to the threshold. Note also that the curve representing the most dangerous mode (the dotted curve) leaves very quickly the stable band obtained from the amplitude equation, but remains permanently inside the stable band of the full calculation. It is worth pointing out that the Eckhaus stable band fits inside the band of nonlinearly allowed states found from steady calculations [5].

Figure 5 shows our results over the tongue, that is, until the planar-front restabilization (the restabilization is reached because the diffusion length becomes of the order of the capillary length).

An important feature of the calculated Eckhaus tongue is that it is strongly tilted. This tilt offers a simple experimental protocol to have access to the phase instability. Indeed a sudden jump of the growth speed should temporarily force the system in the unstable regime. The phase instability should then manifest itself by a large-scale modulation of the interface periodicity leading ultimately to a destruction, or a creation of a new cell, ac-

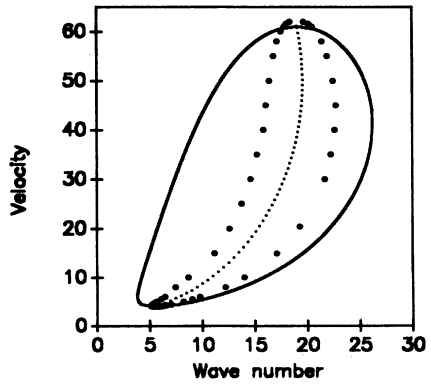

FIG. 5. Same as in Fig. 4, but the results are computed over the tongue, that is, until the planar-front restabilization (units are chosen in such a way that $D=l_T=1$).

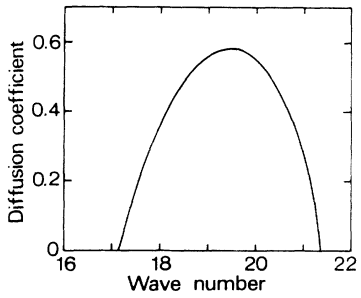

FIG. 6. A typical behavior of the phase-diffusion coefficient as a function of the wave number q (units are chosen in such a way that $D=l_T=1$).

cording to whether the imposed wavelength is too small or too large.

It is worth pointing out, however, that the velocity jump should be sudden enough such that between the initial and final velocity the phase of the pattern does not practically evolve. In other words the phase-diffusion process should be slow enough. Figure 6 shows the phase-diffusion coefficient as a function of the wave number q for a typical velocity ($V=40$). One observes in this figure that the diffusion constant is maximum close to the wave number that provides the fastest growing mode. The average value of the diffusion constant in the stable band is of the order of 1. If one goes back to physical units this means that the phase motion should evolve on a time scale comparable to that of the relaxation of the diffusion field. This time is of the order of D/V^2, which is typically in the range of a second. This makes a rather serious constraint on the velocity jump.

VI. LOCAL DYNAMICS

Since the discovery of the so-called "solitary modes" by Simon, Bechhoefer, and Libchaber [8] during directional growth of a nematic phase at the expense of its isotropic phase, interfacial instabilities have gained a renewed interest. Soon after that discovery it became clear that this mode of growth is a robust feature of various one-dimensional systems [8,11,12,28,29]. Many of these systems have revealed other instabilities, such as "optical modes" (or vacillating-breathing modes). Under some circumstances [12,30–32] the dynamics become apparently irregular, an irregularity which has been tentatively called "chaos." These rich dynamics clearly indicate that the Eckhaus instability is not the only relevant one. Therefore in the hope to achieve a deeper understanding of pattern formation one should perform a full linear stability analysis, and ultimately integrate the full integral equation to study the nonlinear evolution of the instabilities.

In general the equation [e.g., Eq. (8)] that governs the front dynamics involves nonlocal and retarded interactions, which cause difficulties for both analytical and numerical investigations. In particular, it is not *a priori* legitimate to make use of the (very useful) quasistationary approximation, if one is interested in Hopf bifurcations. It is therefore strongly desirable to have at our disposal a more tractable system. We realized that most of the above-mentioned dynamics occur for liquid crystals [32] in a regime where the wavelength of the pattern is significantly larger than the diffusion length; typically $\lambda/l\simeq 10$. We could then expect the front dynamics to be quasilocal. By using a method first devised by Sivashinsky [15] and used by Brattkus and Davis [16] for the one-sided model, we have derived a similar equation appropriate for liquid-crystal systems. We will present below the main lines of the derivation and discuss some of the results. This equation, despite its apparent simplicity, reveals a rich dynamics going from order to chaos, for which we have already given a brief report [17].

The starting point of the derivation of the evolution equation is the determination of the characteristic temporal and spatial scales of the dynamics. This can be done by first performing the linear-stability analysis of the planar front. If one considers fluctuations of the form $e^{iqx+\omega t}$ and uses either Eqs. (1)–(3), (6), or equivalently Eq. (8), we obtain the following dispersion relation:

$$\omega+2=2(1-l_T^{-1}-d_0q^2)(1+q^2+\omega)^{1/2} . \tag{39}$$

The bifurcation is defined by $\omega=0$ and $\partial\omega/\partial q=0$. Using (39), we obtain the critical condition for the onset of the planar-front instability

$$1-l_T^{-1}=3\left[\frac{d_0}{4}\right]^{1/3}-d_0 , \tag{40}$$

and the critical wave number

$$q_c^2=\left[\frac{1}{4d_0^2}\right]^{1/3}-1 . \tag{41}$$

Equation (41) is meaningful only if $d_0\leq\frac{1}{2}$. In the limit $d_0\to\frac{1}{2}$, $q_c^2\to 0$. The limit $d_0\sim\frac{1}{2}$ is the limit of large speeds where the physical capillary length becomes of the order of the diffusion length (recall that the lengths are reduced by the diffusion length $l=2D/V$). We will concentrate on the asymptotic limit where $q_c\to 0$ (that is, when the Péclet number is large). For that purpose we introduce a small auxiliary parameter ϵ defined to be the distance from the "extreme" limit,

$$\epsilon=\tfrac{1}{2}-d_0 . \tag{42}$$

It follows then from Eq. (41) that

$$q_c^2=\tfrac{4}{3}\epsilon+O(\epsilon^2) . \tag{43}$$

Using Eq. (40) we obtain that l_T^{-1} scales as

$$l_T^{-1}=\tfrac{2}{3}\epsilon^2 . \tag{44}$$

Equation (43) shows that the front dynamics is governed in the regime of interest by long-wavelength fluctuations. This means in real space that the front profile is a slowly varying quantity which varies on the scale of $\epsilon^{-1/2}$. Similarly, we can show from Eq. (39) that ω scales as $\omega\sim\epsilon$. In other words, $\omega\sim q_c^2$, which means that the use of the quasisteady approximation [which amounts to neglecting ω in the square root in Eq. (39)] is not legitimate, as could be expected. Now we are in a position to develop the usual multiscale method. That is, we intro-

duce slow space and time variables

$$X=x\sqrt{\epsilon}\ ,\quad T=\epsilon T\ ,\quad Z=z\ . \tag{45}$$

It can be shown that the scale for the front profile is ϵ^0, that is, the calculation to be developed below is valid for order one deformations. We set

$$\zeta\equiv H(X,T)=H_0(X,T)+\epsilon H_1(X,T)+\cdots\ . \tag{46}$$

Similarly, we write the diffusion field as

$$U(X,T,z)=u_0+\epsilon u_1+\cdots\ . \tag{47}$$

Finally, according to (44) we rescale the thermal length as

$$l_T^{-1}=\epsilon^2\bar{l}_T^{-1}\ , \tag{48}$$

where $\bar{l}_T^{-1}$ is a length of order one. Now the scheme is to insert (45) together with (42) and (46)–(48) into the governing equations (1)–(3) and (6) to deduce successively higher-order contributions in power series of ϵ. The calculation is somewhat lengthy but straightforward.

A. Order ϵ^0

To this order we find

$$u_0=\begin{cases} e^{-2(Z-H_0)}\ , & Z>H_0 \quad (49)\\ 0\ , & Z<H_0\ , \quad (50)\end{cases}$$

where H_0 is undetermined at this order.

B. Order ϵ

Expanding Eqs. (1)–(3) and (6) up to order ϵ and using the previous-order results we obtain for the bulk

$$u_1=\begin{cases} De^{-2Z}-\dfrac{F}{2}Ze^{-2Z}\ , & Z>H_0 \quad (51)\\ u_1=C\ , & Z<H_0\ , \quad (52)\end{cases}$$

where

$$F=-2[2H_{0X}^2+H_{0XX}-H_{0T}]e^{2H_0} \tag{53}$$

and where D and C are integration factors depending on the slow variables. Using the interface boundary conditions we obtain

$$C=\frac{H_{0XX}}{2}\ ,\quad D=\frac{FH_0}{2}+[2H_1+C]e^{2H_0}\ . \tag{54}$$

At this order neither H_0 nor H_1 are determined. The really interesting result appears in the next order, where the compatibility condition becomes a constraint for H_0, which is nothing but the evolution equation that we want to determine. The algebra is lengthy, we will simply give the result

$$3H_{0XXXX}-4H_{0XXT}+H_{0TT}+8H_{0XX}+8\bar{l}_T^{-1}H_0=4H_{0X}H_{0XT}+2H_{0XX}H_{0T}-4(H_{0X}^2)_{XX}-2(H_{0X}^3)_X+2H_{0XX}^2\ . \tag{55}$$

Note that this equation is of second order in time. This is a consequence of the nonquasistationary character of the interactions. Indeed the diffusion field evolves on a time scale comparable to that of the interface motion and therefore acts as a feedback on it. As a consequence a "propagative"-type term appears in Eq. (55). Stated in another way the front motion incorporates retardation effects due to the fact that the diffusion does not respond instantaneously; the second time derivative can be thought of as the first expansion of a retardation diffusion kernel.

We note also that the only parameter that remains in Eq. (55) is $\bar{l}_T^{-1}$, which is the inverse of the driving force ($\bar{l}_T^{-1}\sim G/V$; recall that G is the applied thermal gradient).

We have recently shown [17] that Eq. (55) exhibits a rich dynamics: symmetric steady solutions, parity-broken traveling states, vacillating breathing, and chaos. We are planning to report extensively along this line in the near future. Let us here simply point out some simple properties of Eq. (55).

First, by integrating Eq. (55) over a period we obtain that the mean front position obeys for a periodic solution the following inequality:

$$\langle H_0\rangle=\frac{1}{4\bar{l}_T^{-1}}\langle H_{0XX}^2\rangle>0\ . \tag{56}$$

This result is to be contrasted to the one obtained for the one-sided model where $\langle H_0\rangle=0$. In the symmetric model we are considering, the forward advance of the mean position is attributed to the existence of a short circuit of the mass current in the crystalline phase (i.e., the nematic phase). The advance is necessary to guarantee the mass conservation on the global scale.

Another interesting result in this "large"-speed regime is that the physical wavelength of the pattern λ scales with the growth velocity and with the thermal gradient as

$$\lambda\sim\frac{1}{V}f\left[\frac{G}{V}\right]\ . \tag{57}$$

This result follows simply from the fact that in Eq. (55) the lengths are reduced by l and that $\bar{l}_T^{-1}\sim G/V$. This is a purely dimensional analysis. This result contrasts with

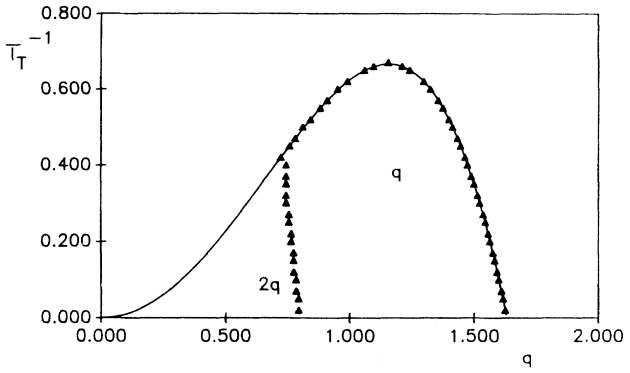

FIG. 7. The full line represents the neutral curve, the symbols delimit the domain of existence of steady-state and symmetric solutions with a fundamental wave number q. At the "vertical" line, represented by triangles to the left, the q family runs into a fold singularity and merges with solutions having $2q$ as a basic wave number.

the one derived in the small-Péclet-number limit [33] where $\lambda \sim 1/\sqrt{V} f(G/V)$. We have computed [34] the domain of existence of steady-state and symmetric solutions inside the neutral curve. Figure 7 shows the results. There exists a continuous family of these solutions delimited by the triangles. For large wave numbers the family extends up to the neutral curve, while for small wave numbers it runs into a fold singularity and merges with solutions having $2q$ as a basic wave number. This event occurs when the $2q$ mode becomes quasineutral, as can easily be checked in Fig. 7 with the help of a rule. A remarkable point is that the wave number q (which is the reduced one) is approximately constant along the fold singularity line, which means that the scaling function in Eq. (57) $f \simeq$const. This entails that the physical wavelength should approximately follow the scaling

$$\lambda \sim 1/V \ . \tag{58}$$

This result is consistent with the observations made in the large-Péclet-number limit where the selected wavelength follows the same scaling [10]. The reason why $f \simeq$const is easy to understand. First we should indicate that this result means that the effect of the thermal gradient on the wavelength of the pattern is extremely weak. This is traced back to the fact that the thermal length scales as $l_T \sim \epsilon^{-2}$ [see Eq. (44)] while the wavelength of the pattern scales on a much shorter length, $\lambda \sim \epsilon^{-1/2}$ [see Eq. (43)]. In other words, $l_T \gg \lambda$ and therefore the interface can be viewed as evolving in a quasi-isothermal environment. The effect of the thermal gradient is then expected to be very weak.

VII. CONCLUSION

We briefly sum up the main lines treated in this paper.

(i) We have given an extensive derivation of the phase-diffusion equation from the front integral equation by making use of a nonlinear WKB method. Our derivation is general and can be extended to the one-sided model, or to situations where diffusion is asymmetric.

(ii) We have confined ourselves to the experimental setup relative to liquid-crystal systems, where the front dynamics is appropriately described by the symmetric model with a constant miscibility gap. Since the regime of the planar-front restabilization has become by now accessible to standard experiments [10,29], we have computed the Eckhaus boundaries inside the tongue where the planar front is unstable. We find that even very close to the Mullins-Sekerka threshold, the actual Eckhaus boundaries strongly deviate from those obtained from the lowest-order Landau-Ginzburg expansion. A remarkable result is that the actual Eckhaus tongue is strongly tilted and inspires a simple experimental protocol for its experimental investigation.

(iii) With the aim to study other types of instabilities, including parity breaking, vacillating breathing, and chaos, we have brought out a simple local equation appropriate for experiments on liquid crystals. This equation has indeed proven to retain many interesting features of interface dynamics. The discovery of a quasiperiodic route into chaos [17] is one of the richnesses of this equation. We are investigating other features of interface dynamics exhibited by this equation, and in particular the transition to spatiotemporal chaos. The preliminary results are promising and we are planning to communicate them in the future.

ACKNOWLEDGMENTS

C.M. acknowledges the "Centre National des Etudes Spatiales" for financial support. C.M. would like to thank A. Valance for his collaboration. The Groupe de Physique des Solides is "Unité de Recherche associée du Centre National de la Recherche Scientifique."

[1] For a recent review, see H. Müller-Krumbhaar and W. Kurz, *Materials Science and Technology* (VCH Verlagsgesellschaft, Weinheim, 1991).

[2] W. W. Mullins and R. F. Sekerka, J. Appl. Phys. **35**, 444 (1964).

[3] W. Kurz and D. J. Fisher, *Fundamentals of Solidification*, 3rd ed. (Trans. Tech., Switzerland, 1989).

[4] P. Oswald, J. Bechhoefer, and A. Libchaber, Phys. Rev. Lett. **58**, 2318 (1987).

[5] L. H. Ungar and R. A. Brown, Phys. Rev. B **29**, 1367 (1984); **30**, 3993 (1984); **31**, 5923 (1985); **31**, 5931 (1985); N. Ramprassad, M. J. Bennett, and R. A. Brown, *ibid.* **38**, 583 (1988); D. Kessler and H. Levine, Phys. Rev. A **39**, 3041 (1989).

[6] Y. Saito, C. Misbah, and H. Müller-Krumbhaar, Phys. Rev. Lett. **63**, 2377 (1989).

[7] A. Classen, C. Misbah, H. Müller-Krumbhaar, and Y. Saito, Phys. Rev. A **43**, 6920 (1991).

[8] A. J. Simon, J. Bechhoefer, and A. Libchaber, Phys. Rev. Lett. **61**, 2574 (1988); M. Rabaud, Y. Couder, and S. Michalland, Eur. J. Mech. B: Fluids **10**, Suppl. 2, 253 (1991).
[9] K. Brattkus and C. Misbah, Phys. Rev. Lett. **64**, 1935 (1990).
[10] J.-M. Flesselles, A. J. Simon, and A. Libchaber, Adv. Phys. **40**, 1 (1991).
[11] G.Faivre, S. de Cheveigné, C. Guthmann, and P. Kurowski, Europhys. Lett. **9**, 779 (1989).
[12] M. Rabaud, S. Michalland, and Y. Couder, Phys. Rev. Lett. **64**, 184 (1990).
[13] P.Coullet, R. Goldstein, and G. H. Gunaratne, Phys. Rev. Lett. **63**, 1954 (1989).
[14] K. Kassner and C. Misbah, Phys. Rev. Lett. **65**, 1458 (1990); **66**, 522(E) (1991); Phys. Rev. A **44**, 6533 (1991); H. Levine and W. Rappel, *ibid.* **42**, 7475 (1990).
[15] G. I. Sivashinsky, Physica D **8**, 243 (1983).
[16] K. Brattkus and S. H. Davis, Phys. Rev. B **38**, 11 452 (1988).
[17] K. Kassner, C. Misbah, and H. Müller-Krumbhaar, Phys. Rev. Lett. **67**, 1551 (1991).
[18] G. E. Nash and M. E. Glicksman, Acta Metall. **22**, 1283 (1974); J. S. Langer, *ibid.* **25**, 1121 (1977).
[19] L. Kramer, E. Ben-Jacob, H. Brand, and M. C. Cross, Phys. Rev. Lett. **49**, 1891 (1982).
[20] See, for example, G. B. Whitham, *Linear and Nonlinear Waves* (Wiley, New York, 1974).
[21] P. G. de Gennes, *Superconductivity of Metals and Alloys* (Benjamin, New York, 1966).
[22] W. Eckhaus, in *Studies on Nonlinear Stability Theory,* Springer Tracts in Natural Philosophy Vol. 6 (Springer, Berlin, 1965).
[23] H. Riecke and H. Paap, Phys. Rev. A **33**, 547 (1986).
[24] K. Kassner and C. Misbah, Phys. Rev. A **44**, 6513 (1991).
[25] C. A. Brebbia, *The Boundary Element Method for Engineers* (Penetech, London, 1978).
[26] Y. Saito, G. Golbeck-Wood, and H. Müller-Krumbhaar, Phys. Rev. A **38**, 2148 (1988).
[27] See, for example, J. P. Keener, *Principles of Applied Mathematics: Transformation and Approximations* (Addison-Wesley, Reading, MA, 1988).
[28] I. Mutabazi, J. Hegset, C. D. Andereck, and J. Wesfreid, Phys. Rev. Lett. **64**, 1729 (1990).
[29] P. Oswald, J. Phys. (Paris) II **1**, 571 (1991).
[30] J. T. C. Lee and R. A. Brown (unpublished).
[31] S. de Cheveigné and C. Guthmann, J. Phys. (Paris) I **2**, 193 (1992).
[32] J. M. Flesselles, A. J. Simon, and A. Libchaber (private communication).
[33] K. Kassner and C. Misbah, Phys. Rev. Lett. **66**, 445 (1991).
[34] This result was mentioned in Ref. [17].